

CHEMISTRY

A European Journal



Accepted Article

Title: Efficient Intersystem Crossing in Tröger's Base Derived From 4-Amino-1,8-Naphthalimide and Application as Potent PDT Reagent

Authors: Yingjie Zhao, Kepeng Chen, Elif Akhuseyin Yildiz, Shujing Li, Yuqi Hou, Xue Zhang, Zhijia Wang, Jianzhang Zhao, Antonio Barbon, Halime Gul Yaglioglu, and Huijian Wu

This manuscript has been accepted after peer review and appears as an Accepted Article online prior to editing, proofing, and formal publication of the final Version of Record (VoR). This work is currently citable by using the Digital Object Identifier (DOI) given below. The VoR will be published online in Early View as soon as possible and may be different to this Accepted Article as a result of editing. Readers should obtain the VoR from the journal website shown below when it is published to ensure accuracy of information. The authors are responsible for the content of this Accepted Article.

To be cited as: *Chem. Eur. J.* 10.1002/chem.201905248

Link to VoR: <http://dx.doi.org/10.1002/chem.201905248>

Supported by
ACES

WILEY-VCH

RESEARCH ARTICLE

Efficient Intersystem Crossing in Tröger's Base Derived From 4-Amino-1,8-Naphthalimide and Application as Potent PDT Reagent

Yingjie Zhao,^{[a],§} Kepeng Chen,^{[a],§} Elif Akhuseyin Yildiz,^[b] Shujing Li,^[c] Yuqi Hou,^[a] Xue Zhang,^[a] Zhijia Wang,^[a] Jianzhang Zhao,^{*,[a]} Antonio Barbon,^{*,[d]} Halime Gul Yaglioglu^{*,[b]} and Huijian Wu^{*,[c]}

Abstract: Intersystem crossing (ISC) was observed for naphthalimide-derived Tröger's base, and the ISC is confirmed as spin orbital charge transfer ISC (SOCT-ISC) mechanism. Conventional electron donor/acceptor dyads showing SOCT-ISC are with semi-rigid linkers. In contrast, the linker between the two chromophores in Tröger's base is rigid and torsion is completely inhibited, which is beneficial for efficient SOCT-ISC. Femtosecond (fs) transient absorption (TA) spectra demonstrated the charge separation and the charge recombination-induced ISC processes. Nanosecond TA spectroscopy confirmed the ISC and the triplet state is long-lived (46 μ s, room temperature). The ISC quantum yield is solvent polarity-dependent (8% ~ 41%). The triplet state were studied with pulsed laser excited time-resolved electron paramagnetic resonance (TREPR) spectroscopy, both NI localized triplet state and ³CT state were observed, which is in good agreement with the spin density analysis. The Tröger's base was confirmed as a potent photodynamic therapy (PDT) reagent with HeLa cells (EC₅₀ = 5.0 nM).

Introduction

Triplet photosensitizers (PSs) have attracted much attention in recent years,^[1,2] for not only fundamental photochemistry studies,^[3] but also for applications in photocatalytic synthetic organic reactions,^[4–7] photodynamic therapy (PDT),^[2] photovoltaics,^[8] and more recently for the triplet-triplet-annihilation upconversion.^[9–11] Triplet PSs are expected to show strong absorption of UV/Vis excitation light, efficient intersystem

crossing (ISC), long-lived triplet state, appropriate redox potentials, and robust photo- and chemostability.^[12] Efficient ISC is one of the crucial characters of the triplet PSs. However, ISC is electron spin-forbidden process, therefore, some driving force must be available to enhance this forbidden process.^[13] The most straightforward method to enhance the ISC in organic compounds is the heavy atom effect. Attaching a heavy atom, for instance, iodine, bromine, or the transition metal atoms (Pt, Ir, Ru, Os, etc) to a chromophore, will enhance the ISC.^[13] However, the heavy atom-containing compounds are normally toxic or the synthesis is costly (e.g. using precious metals such as Pt, Ir, Ru, etc).^[12] Therefore, it is important to devise novel heavy atom-free molecular structural motifs to enhance the ISC.

Driving forces other than heavy atom effect for enhancing ISC has been reported. For instance, molecules with $n-\pi^* \leftrightarrow \pi-\pi^*$ transition are usually known to have efficient ISC (El-Sayed rule).^[13] Exciton coupling may also enhance ISC, this mechanism is based on the energy level splitting and the matching of the S₁/T_n states.^[14] Charge recombination (CR) induced ISC was also reported for the electron donor/acceptor dyads, based on the radical-pair ISC (RP-ISC) mechanism.^[15,16] Recently the electron spin converter strategy was also reported.^[17,18] Radical enhanced ISC based on electron spin exchange interaction was also studied.^[19,20] However, various drawbacks exist for these approaches, e.g., the synthesis of the molecules is demanding, or ISC kinetics is slow and the ISC efficiency is unsatisfactory.

Recently, the spin orbital charge transfer ISC (SOCT-ISC) in compact electron donor/acceptor dyads has attracted much attention.^[21–25] In these dyads the linker between the electron donor and acceptor is short, it can be a C–C or C–N single bond, which is different from the conventional electron donor/acceptor dyads showing RP-ISC, in which a long and rigid linker between electron donor and acceptor has to be used to reduce the electron exchange values (the exchange interaction, J , should be much smaller than 1 cm⁻¹), thus to make the RP-ISC possible.^[16] Moreover, in the SOCT-ISC dyads, the electron donor/acceptor adopt orthogonal geometry, so that the electron transfer is accompanied with molecular orbital angular momentum change, which compensates the electron spin angular momentum change of the ISC process. As a result, the ISC can be enhanced by electron transfer between the perpendicularly orientated electron donor/acceptors.

One critical issue for the molecular design of the SOCT-ISC triplet PS is implementation of the molecular geometry restriction to attain the orthogonally aligned electron donor and acceptor. Previously, in a julolidine-anthracene dyads, methyl groups were introduced to the ortho-position of the linkers to enhance the molecular conformation restriction.^[21] The 1,7-methyl groups on

[a] Y. Zhao, K. Chen, Y. Hou, X. Zhang, Dr. Z. Wang and Prof. J. Zhao State Key Laboratory of Fine Chemicals, School of Chemical Engineering, Dalian University of Technology, E-208 West Campus, 2 Ling Gong Road, Dalian 116024, China. E-mail: zhaojzh@dlut.edu.cn (J. Z.)

[b] Dr. A. Yildiz, Prof. G. Yaglioglu Department of Engineering Physics, Faculty of Engineering, Ankara University, 06100 Beşevler, Ankara, Turkey. E-mail: yoglu@eng.ankara.edu.tr (G. Y.)

[c] S. Li and Prof. H. Wu School of Bioengineering & Key Laboratory of Protein Modification and Disease, Liaoning Province, Dalian University of Technology, Dalian, China. E-mail: wuhj@dlut.edu.cn (H. Wu)

[d] Dr. A. Barbon Dipartimento di Scienze Chimiche, Università degli Studi di Padova, Via Marzolo 1, 35131 Padova, Italy. E-mail: antonio.barbon@unipd.it

§ Y. Z. and K. C. contribute equally to this work.

Supporting information for this article is given via a link at the end of the document.

RESEARCH ARTICLE

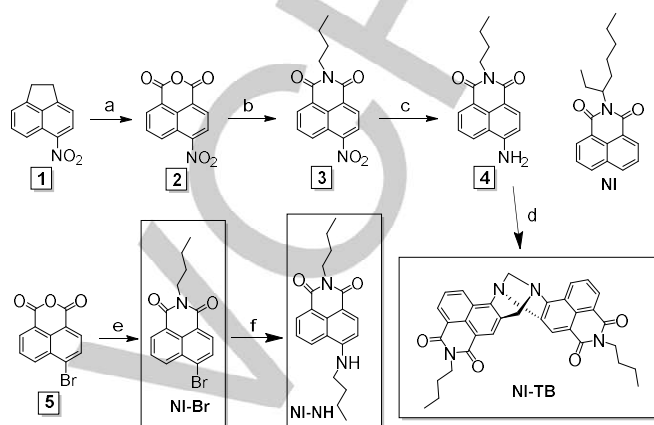
the Boron dipyrromethene (Bodipy) moiety play the similar role in the Bodipy-derived electron donor/acceptor dyads showing SOCT-ISC.^[22,23,26] We found that the presence of *peri*-H (C) of electron donor phenothiazine is helpful for conformation restriction.^[24,27,28] However, in all these molecular structural motifs, the rotation about the C–C or the C–N linker is not fully restricted, and various conformations are still accessible with the thermal energy. Deviation from the orthogonal geometry may be detrimental to the SOCT-ISC efficiency. As such, fully rigid linker is desired for linking the electron donor/acceptor in these dyads, but this kind of linker is difficult to attain from a point of view of synthesis.

Concerning this aspect, we noted the potential of the unique molecular structure of Tröger's base to enhance the SOCT-ISC. Tröger's bases, which have been known for decades, are cleft-shaped molecules containing a diazocine ring to connect two chromophores.^[29] Tröger's bases have played a considerable role in supramolecular chemistry, in the areas of molecular recognition, molecular separation, and photoswitches,^[30–33] or as hole transport materials for OLED.^[34] The most intriguing feature of these molecules to us, is the fully rigid, and the almost perpendicular geometry of the two aromatic moieties (90 ~ 104 °). These features are beneficial for the purpose of attaining SOCT-ISC. However, the ISC of Tröger's bases was not reported. In 2005, Lewis et al. reported the naphthalimide (NI)-derived Tröger's base.^[35] The red-shifted and quenched fluorescence in polar solvent were noted, but the non-radiative decay mechanism in polar solvents was not studied in detail.^[35] Gunnlaugsson et al. made a detail study on the luminescence imaging and photocleavage of DNA and sensing of explosives with the naphthalimide (NI)-derived Tröger's base.^[36–38] Although it is known that the photocleavage of DNA is usually due to generation of reactive oxygen species (ROS) by the intercalator, for instance, singlet oxygen (¹O₂) or superoxide radical anion (O₂^{•-}),^[39,40] yet the ISC of Tröger's bases was not reported. Recently a NI-derived Tröger's base–Ru(II)–curcumin organometallic conjugate was demonstrated to show cytotoxicity against cervical cancer cells, but the phototoxicity and the ISC of the base of itself were not studied.^[41]

Based on these previous studies on Tröger's bases, i.e. the quenching of the fluorescence in polar solvents and the orthogonal geometry, we suppose that SOCT-ISC may occur in Tröger's bases, via the symmetry-breaking CT (SBCT), i.e. one NI moiety acts as the electron donor and another NI moiety in the Tröger's base acts as electron acceptor.^[42]

Herein we propose to use the rigid, almost orthogonal geometry of the two subunits in Tröger's base to implement the SOCT-ISC. Due to its excellent photophysical property and stability, we selected the NI moiety as the visible light-harvesting chromophore to prepare the Tröger's base. We studied the photophysical properties of the **NI-TB** with various steady state and time-resolved transient spectroscopies. Photo-induced electron transfer was confirmed with femtosecond transient absorption spectroscopy (fs TA). The formation of the triplet excited state was confirmed with nanosecond transient absorption (ns TA) spectroscopy. Time-resolved electron paramagnetic resonance (TREPR) spectroscopy was also used

to study the ISC mechanism and the electron spin polarization (ESP) of the triplet state in detail. PDT effect of **NI-TB** was studied as well. These results are helpful for development of novel molecular motifs for attaining efficient ISC in heavy atom-free organic compounds as well as for application of these novel triplet PSs in photocatalysis and photon upconversion, etc.



Scheme 1. Synthesis of **NI-TB**. (a) Na₂Cr₂O₇·2H₂O, AcOH, reflux, 5 h, under N₂, yield: 57%; (b) *n*-C₄H₉NH₂, EtOH, reflux, 2h, under N₂, yield: 56%; (c) SnCl₂·2H₂O, Con. HCl, EtOH, RT, 15 min, yield: 85%; (d) paraformaldehyde, CF₃COOH, RT, 9 h, under N₂, yield: 73%; (e) similar to step (b), yield: 91%; (f) *n*-C₄H₉NH₂, CH₃OCH₂CH₂OH, reflux, 8 h, under N₂, yield 63%.

Results and Discussions

Conventional Tröger's bases are normally with substituted benzene ring as the chromophore, which show absorption in UV spectral region.^[29] Clearly this is a disadvantage for most of the applications, which normally require absorption in visible spectral region. We considered the NI-derived Tröger's base as a candidate for triplet PSs based on SOCT-ISC,^[31,35–38] in which the NI moiety show absorption in visible region. Thus we studied the possible ISC of the NI-derived Tröger's base. The preparation of the **NI-TB** (Scheme 1) is based on the reported method,^[37] and the molecular structure of the target compounds was fully verified with ¹H NMR and HR MS spectra (see Experimental Section).

The UV–Vis absorption spectra of some of the compounds presented in Scheme 1 were studied (Figure 1). **NI-Br** shows a structured absorption spectrum, with vibronic bands centered at

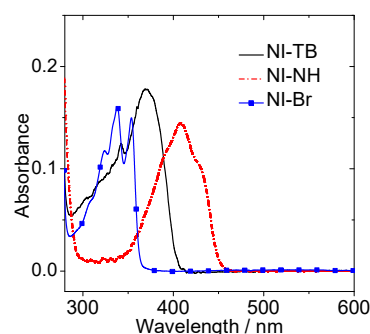


Figure 1. UV–Vis absorption spectra of **NI-NH**, **NI-TB** and **NI-Br**. *c* = 1.0 × 10⁻⁵ M in *n*-hexane. 25 °C.

RESEARCH ARTICLE

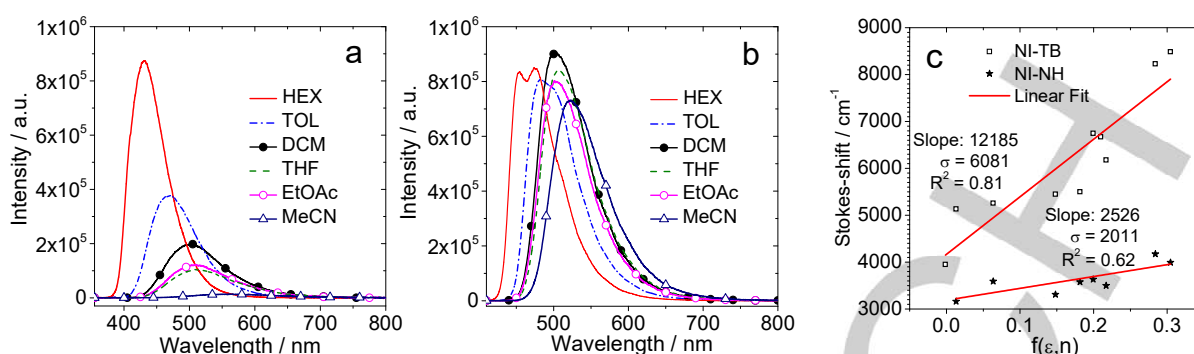


Figure 2. Fluorescence emission spectra of (a) **NI-TB** in different solvents ($\lambda_{\text{ex}} = 345$ nm, $A = 0.137$) and (b) **NI-NH** in different solvents ($\lambda_{\text{ex}} = 400$ nm, $A = 0.132$); Optically matched solutions were used (the concentration is varied slightly to attain the same absorbance at the excitation wavelength). (c) Lippert-Mataga plots for **NI-TB** (the coefficient of determination $R^2 = 0.81$, the estimated standard deviations $\sigma = 6081$) and **NI-NH** ($R^2 = 0.62$, $\sigma = 2011$ for the fitting); $f(\epsilon, n) = [(\epsilon - 1)/(2\epsilon + 1) - 0.5 \times (n^2 - 1)/(2n^2 + 1)]$. The solid lines are the fitting results. The solvents used are: *n*-hexane, toluene, toluene : DCM (4/1, v/v), THF, ethyl acetate, MeCN, CHCl₃ and acetone, in the order of increasing f values. 25 °C.

324 nm, 338 nm and 354 nm, respectively. With amino group attached on the 4-position of the NI moiety, **NI-NH** shows broad, strongly red-shifted and structureless absorption band centred at 408 nm. It indicates the lone pair electrons of the amino group are in π -conjugation with the NI unit, and the electronic push-pull interaction (i.e. intramolecular charge transfer, ICT) between the amino group and NI unit is strong. However, for **NI-TB**, a broad band at 370 nm was observed. The main absorption band at 370 nm is blue-shifted as compared to **NI-NH** (408 nm). The absorption feature of **NI-TB** studied herein is in agreement with those of the NI-based Tröger's base reported previously.^[31,37]

The red-shifted broad absorption of **NI-TB** as compared to **NI-Br** is not resulted from the exciton coupling between the two NI units.^[43] The red-shifted and broadened absorption band is attributed to the ICT effect in **NI-TB**, because the amino groups are not fully decoupled from the NI moiety, which is similar to **NI-NH**, although in minor extent. This is also in agreement with the results obtained for the phenyl derived Tröger's base.^[44]

It is interesting that the absorption of **NI-TB** is blue-shifted as compared to **NI-NH**, which indicates that the lone pair of the N atom in the bridge of **NI-TB** do not fully participate in the π -conjugation system as compared to **NI-NH**, we assign this limited π -conjugation to the conformation restriction in **NI-TB** by the rigid diazocine linker between the two NI units.^[45] By changing the polarity of the solvent, bathochromic effect for the absorption bands of **NI-TB** and **NI-NH** was observed (Supporting Information, Figure S7).

The fluorescence emission of **NI-TB** and **NI-NH** were studied (Figure 2). For **NI-TB**, a broad fluorescence emission band was observed in most of the solvents used. The emission band is red-shifted, the intensity is reduced with increasing solvents polarity. These behaviour is typical for emission from a charge transfer state.^[46] However, for **NI-NH**, with the solvent polarity increased, the emission band is only slightly red-shifted, and no substantial change was observed for the emission intensity (Figure 2b), indicating that the ICT effect in the two compounds is different. This is interesting, because the UV-Vis absorption studies show that the π -conjugation of the amino N atom is less efficient in **NI-TB** than that in **NI-NH** at ground state (Figure 1), thus the solvent

polarity-dependency of the fluorescence of **NI-TB** should be weaker. Based on these results, we propose there is CT between the two NI units in **NI-TB** upon photoexcitation. Previously it was shown that the linker of the two chromophore in Tröger's base molecule, i.e. methano-1,5-diazocine ring, is efficient for shift of the electron/hole in the molecules.^[47]

To further investigate the excited state dipole moment changes of **NI-TB** and **NI-NH** upon photoexcitation, the effect of the solvent polarity on the CT emission band were studied in detail, and the data were analyzed with the Lippert-Mataga plots (Figure 2c).^[46] Linear plots observed for the two compounds indicated the general solvent effect.^[48] The dipole moments of the S₁ state of two compounds are obtained as μ_e (**NI-TB**) = 21.0 D, μ_e (**NI-NH**) = 9.1 D, based on the ground state dipole moment μ_g (**NI-TB**) = 4.8 D and μ_g (**NI-NH**) = 6.0 D, approximated from the ground state geometry optimization by DFT calculation. The charge separation distance of two compounds are approximated as d (**NI-TB**) = 4.3 Å and d (**NI-NH**) = 1.9 Å by the equation $\mu = q \times d$, assuming one unit of charge is separated completely in the molecules. Note the optimized ground state geometry indicates that the centroid-to-centroid distance of the two NI units in **NI-TB** is ca. 7.3 Å; the distance between the bridging methylene carbon to the NI center is ca. 4.8 Å. The charge separation distance of **NI-TB** is about twice than that of **NI-NH**, which rationalize the larger dipole moment changes upon photoexcitation. Thus we propose that symmetry breaking CT occurs in **NI-TB**,^[46] which is different from the normal ICT in **NI-NH** (N atom in amino group as the electron donor).^[49,50] Previously the fluorescence of a carboxylate ester-attached benzene derived Tröger's base was studied with the Lippert-Mataga plot, and it was found that the dipole moment change upon excitation is up to 14.79 D.^[44]

The fluorescence lifetime of **NI-TB** decreases in more polar solvents, i.e., from *n*-hexane (8.0 ns) to MeCN (1.6 ns, Supporting Information, Figure S8a). One reason is the energy gap law, i.e. the smaller energy gap of S₁/S₀ in polar solvent makes the non-radiative decay of S₁ state prevail.^[46] However, for **NI-NH**, the fluorescence emission lifetime prolongs with increasing of the solvent polarity (Figure S8b), e.g. the fluorescence lifetime increased from 7.7 ns (in hexane) to 12.8 ns (in MeCN). These results indicated that the bright state of **NI-NH** is with twisted

RESEARCH ARTICLE

intramolecular charge transfer (TICT) character,^[45] especially in polar solvents. It also indicates the solvent polarity-dependency of the CT fluorescence bands in **NI-TB** and **NI-NH** is different, i.e., the ICT effect of two compounds is different. The photophysical parameters of the compounds are summarized in Table 1 (refer to Supporting Information, Table S1 for more information on the fluorescence lifetimes).

Table 1. Photophysical properties of the compounds.

	Solvent [a]	λ_{abs} [b]	ϵ [c]	λ_{em} [d]	Φ_{F} [e]	τ_{F} [f]	μ [g]
NI-TB	HEX	369	1.78	431	0.84	8.0	21(¹ CT) 4.8(S_0)
	DCM	384	1.85	500	0.28	6.5	
	MeCN	382	1.77	563	0.02	1.6 (98%) 13.2 (2%)	
NI-NH	HEX	408	1.06	476	0.61	7.7	9.1(¹ CT) 6.0(S_0)
	DCM	427	1.13	502	0.52	11.2	
	MeCN	433	1.19	522	0.58	12.8	

[a] HEX, DCM and MeCN stand for *n*-hexane, dichloromethane and acetonitrile, respectively. The $E_{\text{T}}(30)$ values are *n*-hexane (31.0), DCM (40.7) and MeCN (45.6). [b] The maximum absorption wavelength, in nm. [c] The molar extinction coefficient at the absorption maxima, in $10^4 \text{ M}^{-1} \text{ cm}^{-1}$. [d] The maximum fluorescence emission wavelength, in nm. [e] Fluorescence quantum yield, with anthracene as the standard ($\Phi_{\text{F}} = 0.30$ in ethanol). [f] The fluorescence lifetime, in ns. [g] The dipole moment of the states.

The singlet oxygen quantum yields (Φ_{Δ}) of **NI-TB** is solvent-dependent (Supporting Information, Table S2). Highest value was observed in DCM ($\Phi_{\Delta} = 41\%$), moderate values were observed in toluene ($\Phi_{\Delta} = 21\%$) and THF ($\Phi_{\Delta} = 22\%$), Φ_{Δ} is much smaller in other solvents. In comparison, **NI-NH** shows negligible Φ_{Δ} values.

The triplet state formation was studied by nanosecond transient absorption (ns TA) spectra of **NI-TB** (Figure 3). In the ns TA transient absorption spectra, the typical absorption band of $^3\text{NI}^*$ state at 480 nm was observed and the triplet state lifetime was determined as 46 μs (in deaerated DCM). In aerated solution, the lifetime was quenched to 0.7 μs (Supporting Information, Figure S12d). Due to the ground state bleaching band of **NI-TB** at around 370 nm, which overlaps with the ESA band in this range, the typical ESA band of the triplet state of NI moiety at 390 nm was not observed for **NI-TB**, but a new ESA band at 600 nm was observed for **NI-TB** as compared to **NI-Br** (Supporting Information, Figure S11a). The charge separation (CS) upon photoexcitation was confirmed with femtosecond transient absorption spectroscopy (Supporting Information, Figure S17a), indicated by the absorption band at 435 nm (NI radical anion absorption, $\text{NI}^{\cdot-}$). It should be pointed out that the absorption of the cation may be much weaker, or overlapped with the absorption of anion, therefore no distinct cation absorption was observed in fs TA spectra, subsequently, fs TA spectra show that a species with ESA at 480 nm was produced, which is assigned to the NI triplet state. With global fitting of the fs TA data, the CS time constant

was determined as 0.3 ps, and the charge recombination takes ca. 3 ns to give the NI localized triplet state.

The ISC of the compounds was studied with pulsed laser excited time-resolved electron paramagnetic resonance (TREPR) spectroscopy (Figure 4). TREPR is a unique and powerful spectroscopy to detect spin unpaired electrons and to study the triplet state and electron spin polarization (ESP) dynamics.^[51] It has been used for study the ISC mechanisms,^[21,52] as well as the confinement of the triplet state wave function.^[53,54]

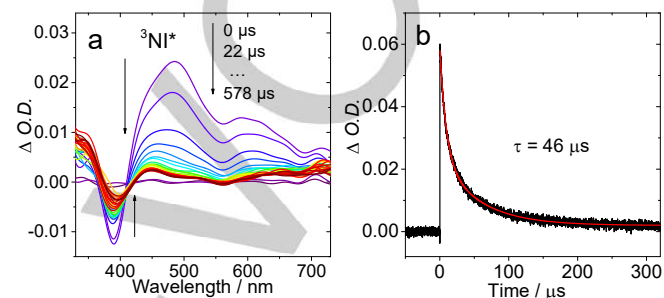


Figure 3. Nanosecond transient absorption spectra of **NI-TB**. (a) the spectra in absence of TEA and (b) corresponding decay trace at 480 nm. c **NI-TB** = $5.0 \times 10^{-5} \text{ M}$ in deaerated DCM. Excitation was realized with a nanosecond pulsed laser at 355 nm. 25 °C.

It is known that NI moiety itself shows efficient ISC ($\Phi_{\text{T}} = 92\%$).^[55] Thus we need to clarify that the ISC of **NI-TB** is not due to this intrinsic ISC of NI moiety. TREPR spectroscopy is able to discriminate paramagnetic states produced by different mechanisms. Mostly, triplet states and radicals are observed with TREPR spectroscopy. Here we observed triplet states, with different magnitude of the interaction between the electrons. For formation of triplet states, the spin-orbit coupling ISC (SO-ISC), the radical pair ISC (RP-ISC), and the SOCT-ISC mechanisms,^[16] are able to produce a specific selective population rates of the sublevels of the T_1 state, either for the zero-field splitting (ZFS) states or the high-field Zeeman sublevels, thus specific ESP pattern may develop for different ISC mechanisms. As such the ESP of the TREPR spectrum of the triplet states give information on the triplet state formation mechanism. On the other hand, the ZFS parameters D and E values obtained from the simulation of the TREPR spectra are useful for discrimination of the ^3CT and the ^3LE states,^[51,56-60] i.e. the confinement of the triplet state wave functions.

The TR-EPR spectra of **NI-Br** and of **NI-TB** were studied at 80 K, in frozen solution (Figure 4). For **NI-Br**, a TREPR spectrum with ESP pattern of *eee/aaa* was observed (Figure 4a). The TREPR spectrum of **NI-Br** is composed of one species, and a prevalent population of the X state (the Y state is also populated. Supporting Information, Table S4). The ESP is that derived from SO-ISC. The theoretical computations on **NI-Br** with the wave function obtained by a HOMO-LUMO excitation (localized on the NI plane) reproduce the experimental ZFS parameters very well (Supporting Information, Table S4). For **NI-TB**, more complicated

RESEARCH ARTICLE

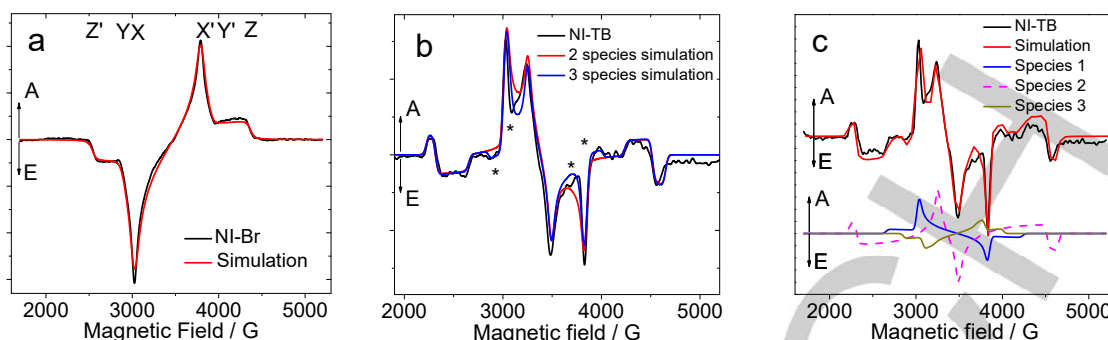


Figure 4. The TR-EPR spectra of **NI-Br** and **NI-TB** obtained at about 1 μ s after a laser flash of 3×10^{-5} M solution in toluene/MeTHF (3:1, v/v) at 80 K. (a) **NI-Br** upon photoexcited at 355 nm (3.5 mJ per pulse) and (b) **NI-TB** irradiated at 355 nm (3 mJ per pulse). The red lines are the simulation curves whose fitting parameter are presented in Table 4. For **NI-TB**, the blue curve is the simulation with three species, and the red curve is the simulation with two species A+B). (c) The simulation with three species curves of (b) and each species were presented, respectively.

TREPR spectrum was obtained (Figure 4b). Satisfactory simulation can be obtained with the sum of three species; by comparison with the calculation conducted for **NI-NMe** (Supporting Information, Table S4 as a **NI-TB** monomer, $D = 895$ G), we assign species A ($D = 795$ G) as a triplet state localized on one of the two NI units (likely, the 100 G D -reduction is due to a perturbation from the other π -system, or spreading of the spin density to the bridge amino moiety). With respect to **NI-Br**, the population of the substrates are rather different, with the X-state the most populated one in **NI-Br**, and no population along Z direction ($P_X : P_Y : P_Z = 1 : 0.5 : 0$), whereas for **NI-TB**, the Z-state is the most populated one ($P_X : P_Y : P_Z = 0.65 : 0 : 1$, Supporting Information, Table S4). This observation supports our hypothesis that the population of the triplet state in **NI-TB** is not via a regular SO-ISC, which shows a population mainly of the X-state (the same holds for the NDI molecule). The RP-ISC mechanism can be excluded as well, which selectively populates the high-field Zeeman states and produces (for $D > 0$) a typical *aeae* pattern.^[55]

We also observed a state with smaller ZFS parameters (species B) for **NI-TB**, e.g. with a substantial smaller D -value (ca. 260 Gauss smaller than species A), which is compatible with the formation of a CT state, characterized by a well distributed wave function for both electrons, having more significant localization on the NI unit, the other on the bridging nitrogen atoms, proposed by the spin density surface of the radical anion and cations of **NI-TB**, Figure 5). We calculated the average distance between the two electrons under a point-dipole approximation, assuming that this state originates from a CT state, thus with the distribution function of the two electrons spatially separated. In this case we obtained an average distance of 0.38 nm for the two spin unpaired electrons, which is in good agreement of the bridging N atom–centroid C atom of the NI core distance (0.38 nm. Based on optimized ground state geometry). Involvement of the bridge amino moiety in this triplet state was also supported by the calculation of the D values of the CT state, the magnitude of the calculated D values indicate that the species B is neither a triplet state localized on one NI unit, nor fully delocalized CT state on two NI units (see Supporting Information, Table S4). We are not clear about the origin of the third species (C) at the moment. It

might be related to the ESA band at 600 nm in the ns TA spectrum. The Z-values indicates it is similar to a distribution of naphthalene, thus further localized. DFT calculation have proven a localization for the T_4 state. T_4 is energetically accessible from the S_1 state, therefore, a possibility is that the observed triplet is a T_4 state. At low temperature the CR, or even the internal conversion of multi-chromophore compounds can be slowed down.^[60] No quintet state spectrum was observed, indicating that the triplet state is confined on one NI unit in **NI-TB** (the two NI units are not in triplet excited state simultaneously).

The dihedral angle between the two NI units in **NI-TB** was found to be 80° in the optimized ground state geometry (Figure 5a), which is similar to the X-ray crystal structure results reported previously (89.17°).^[37] Thus in principle the SOCT-ISC can be enhanced with this geometry. The N–CH₂–N angle in the bridge part was found to be 111.16° and the bond length of the N–C bond in the bridge was 1.463 Å in the optimized ground state geometry, which are very close to those determined with the X-ray diffraction of single crystal (111.84° and 1.463 Å, respectively).^[37] It indicates the basis sets and the function (B3LYP/6-31G (d)) used herein in our study for the theoretical computation are convincing.

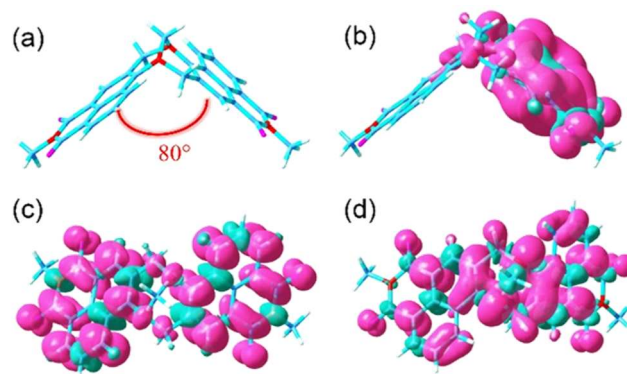
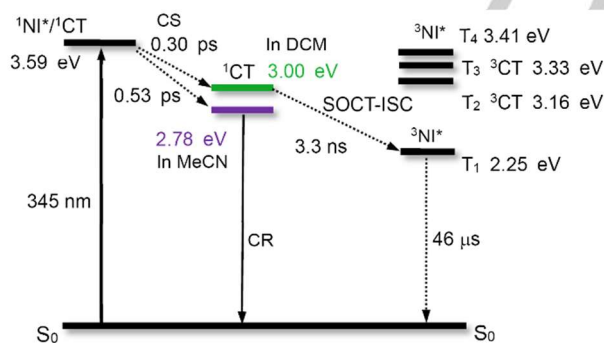


Figure 5. (a) Optimized ground state geometry of **NI-TB** showing the dihedral angle between two moieties (80°); (b) Isosurface of spin density of **NI-TB** at the optimized triplet state (T_1); Isosurface of spin density of (c) **NI-TB** radical anion at the optimized doublet state (D_0) geometry and (d) **NI-TB** radical cation at the optimized doublet state (D_0) geometry. Isovalues = 0.0004. The calculations were performed at the (U)B3LYP/6-31G (d) level using Gaussian 09W.

RESEARCH ARTICLE

The triplet state spin density of **NI-TB** is mostly localized on one of the NI moiety with a little delocalization on the bridge (Figure 5b). It is in agreement with the ns TA spectra of **NI-TB** (Figure 3a), for which the absorption of the NI triplet state is different from that of **NI-Br**. The spin density of the triplet state of Tröger's base also spread to the bridge in the Tröger's base. This slightly delocalized ^3LE state was also confirmed by the TREPR spectrum of **NI-TB** (species A, with *D* and *E* values of 795 and 10 G, respectively). Note the *D* parameters is smaller than that of **NI-Br**, *D* = 915 G). It should be noted that two degenerated triplet states were observed with TDDFT computations, localized on the two NI units, respectively. This is reasonable since the two units are essentially the same.

The spin density of **NI-TB** radical anion and cation were also investigated (Figure 5c and 5d). For radical anion, most of spin density is localized on two NI unit with a little part distributed on the *N* atom of the bridge. It indicates the electron affinity ability of NI unit. However, for radical cation, the spin density is delocalized on the molecule with significant distribution on the bridge part. This computation is in agreement with a previously reported triarylamine-derived Tröger's base, for which the spin of the radical cation is symmetrically delocalized between the two arylamine moieties (confirmed with EPR spectra).^[47] Moreover, the bridge nitrogen atoms contribute significantly to the spin density. This theoretical prediction was also confirmed by the observation of the ^3CT state with TREPR (Figure 4b and Supporting Information, Table S4). Moreover, either the CT with the bridge amino moiety as electron donor, or the CT between the two NI moieties, constitutes a SOCT feature because the molecular orbitals involved in these CT processes are non-coplanar.



Scheme 2. Simplified Jablonski diagram illustrating the photophysical processes of **NI-TB**. Note: The CT excited states denote the (NI⁺-NI⁻) excited state. The energy levels of the ^1CT excited state were approximated from the blue edge of the fluorescence emission peak in different solvents. The energy level of T_n excited states was obtained from the TDDFT calculation based on the optimized geometry of the ground state, the assignment of the ^3CT or ^3LE state of the T_n state is based on NTO orbital analysis. Some T_n states, include T_1 are degenerated, but not shown in the Scheme. The calculations were performed at B3LYP/6-31G (d) level using Gaussian 09W.

The photophysical processes of Tröger's base **NI-TB** are summarized in Scheme 2. Upon photoexcitation, the S_1 state is populated (note this is a mixed $^1\text{NI}/^1\text{CT}$ state, based on the UV-Vis absorption, and the TDDFT computations, Supporting

Information, Figure S24). Then CS occurs (time constants are 0.3 or 0.53 ps, in DCM or ACN, respectively). The amino units and the NI unit act as electron donor (Figure 5). The large dipole moment of the S_1 state of **NI-TB** also infer that there is charge separation between the two NI units within the Tröger's base, thus we propose a SBCT occurs for **NI-TB**. Then a slow CR (ca. 3.3 ns in DCM) produces the $^3\text{NI}^*$ state.

Applications of novel heavy atom-free PSs, for instance, the radical-containing triplet PSs, orthogonal Bodipy dimers in PDT have attracted much attention.^[53,61] Herein we demonstrated that Tröger's base **NI-TB** shows efficient SOCT-ISC (Φ_{Δ} = 41% in DCM). As such we explored its potential application in PDT towards cancer cells (Figure 6). Confocal microscopy was conducted after HeLa cells were incubated with Tröger's base (**NI-TB**) (0.11 μM) for 24 hours (Supporting Information, Figure S21), which shows that the **NI-TB** can be uptakes by the HeLa cells. Then the cell viabilities with and without photoirradiation were determined using a standard MTT assay (Figure 6). Even at very low concentrations of Tröger's base, a significant decrease of the cell viability was observed with a remarkable the lowest half concentration of maximal inhibitory (EC_{50}) value (5.0 nM). The photocytotoxicity of the Tröger's base was demonstrated. In

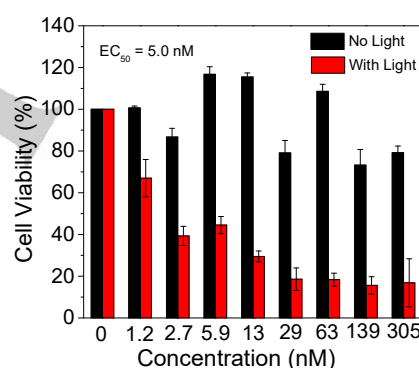


Figure 6. MTT assay of **NI-TB** with different concentrations. Comparison of the cell viability of HeLa cells pre-treated with increasing doses of **NI-TB** with (365 nm, 0.7 mW/cm², 30 min, i.e. the irradiation dose is 1.26 J/cm²) and without light irradiation. 20 °C.

comparison, no significant change was observed when the cells were kept in the dark, in the presence of the same concentration of the Tröger's base (Black bars). Thus, our studies demonstrated a Tröger's base as a novel efficient singlet oxygen PS with a potential applications in photodynamic therapy. In comparison, the heavy atom-free Bodipy dimer triplet PSs show EC_{50} of 50 nM.^[63] Concerning the EC_{50} value, **NI-TB** is also more potent than the iodinated cyanine triplet PSs (EC_{50} = 25 μM),^[62] or brominated Bodipy sensitizers.^[63] The potent PDT activity of **NI-TB** may be attributed to its tight binding ability with DNA.^[32-34] Preparing of Tröger's base showing red and near IR light absorption is in progress in our laboratory.

Conclusion

In conclusion, we observed efficient intersystem crossing (ISC) for a Tröger's base, which is derived from naphthalimide (NI) chromophore, and the unique structure of Tröger's base is

RESEARCH ARTICLE

proposed as a new molecular structural platform for design heavy atom-free triplet photosensitizers. Solvent polarity-dependent singlet oxygen ($^1\text{O}_2$) photosensitizing was observed, with quantum yields (Φ_{Δ}) of 8% ~ 41%. With steady state and femtosecond/nanosecond transient absorption spectroscopies, as well as pulsed laser excited time-resolved electron paramagnetic resonance (TREPR) spectroscopy, we demonstrated that the ISC mechanism is the spin orbital charge transfer intersystem crossing (SOCT-ISC). Conventional electron donor/acceptor dyads showing SOCT-ISC are with semi-rigid linker between the electron donor and acceptor units, very often torsion (rotation) about the linker is not fully inhibited, which is detrimental to the SOCT-ISC efficiency; moreover, the electron donor and acceptor moieties are usually different. Different from those conventional compact donor/acceptor dyads, two same chromophores are used in Tröger's base (one is electron donor and another as electron acceptor), and the linker between the two chromophores in Tröger's base is fully rigid, torsion about the linker is completely inhibited. This conformation restriction is beneficial for attaining efficient SOCT-ISC. UV-Vis absorption spectroscopy shows a very weak π -conjugation between the *N* atom of the amino moiety with NI unit in **NI-TB**, due to the molecular conformation restriction. Fluorescence study shows that a highly polar emissive charge transfer state (CT) was formed, formed via the symmetry-breaking charge transfer. Nanosecond transient absorption spectra indicated the formation of triplet state (T_1 state lifetime is up to 46 μs). Both localized ^3NI state and delocalized ^3CT state were observed in TREPR spectra. The ^3NI state of the Tröger's base shows different sublevel population rates ($p_x : p_y : p_z = 0.65 : 0 : 1$) as compared to that of 4-bromonaphthalimide ($p_x : p_y : p_z = 1 : 0.5 : 0$), for which the ISC is via the normal spin-orbit coupling (SO-ISC). Photodynamic therapy studies with HeLa cells was carried out, high phototoxicity was observed for the Tröger's base (EC_{50} : 5.0 nM). Our results show that the Tröger's bases can be developed as a novel molecular structural platform for heavy atom-free triplet photosensitizers showing efficient ISC.

Experimental Section

General: All the chemicals used in synthesis are analytically pure and were used as received. Solvents were dried and distilled prior to use. The UV-Vis absorption spectra of compounds were recorded on a UV2550 spectrometer (Shimadzu Ltd., Japan). The fluorescence emission spectra were performed on a FS5 fluorescence spectrometer (Edinburgh Instruments, U.K.). The fluorescence lifetimes of compounds were measured on an OB920 luminescence lifetime spectrometer (Edinburgh Instruments, U.K.). The nanosecond transient absorption spectroscopy was recorded with LP980 laser flash photolysis spectrometer (Edinburgh Instrument, U.K.). For other experimental procedures, refer to the Supporting Information.

Time-resolved electron paramagnetic resonance spectroscopy (TREPR) and calculation of the ZFS parameters: Time resolved EPR measurements were conducted at low temperature inside a CF935 cryostat (Oxford) cooled by liquid nitrogen. A Bruker ELEXSYS spectrometer was used for the acquisition of the EPR time trace, following a laser flash, under direct detection mode. We used an MD5 dielectric cavity, characterized by a response time of about 0.5 μs . Excitation was performed by a Quantel Rainbow laser equipped with second, third harmonics, and OPO for irradiation at different wavelength in the visible

region. The ZFS principal directions and principal values were calculated from a simple HOMO-LUMO excitation under the point dipole approximation,^[64–66] where the molecular orbital wave functions were computed by the AM1 method, as implemented in the MOPAC code.^[67]

Acknowledgements

J. Z. thanks the NSFC (21673031, 21761142005, 21911530095 and 21421005), the Fundamental Research Funds for the Central Universities (DUT2019TA06) and State Key Laboratory of Fine Chemicals (ZYT201901) for financial support. The support from Dipartimento di Scienze Chimiche, Università degli Studi di Padova for academic visit of J. Z. is also gratefully acknowledged.

Keywords: Intersystem Crossing • Naphthalimide • Triplet state • Tröger's base • Electron Spin Polarization • Photodynamic therapy

- [1] X. Li, S. Kolemen, J. Yoon, E. U. Akkaya. *Adv. Funct. Mater.* **2017**, *27*, 1604053–1604064.
- [2] A. Kamkaew, S. H. Lim, H. B. Lee, L. V. Kiew, L. Y. Chung, K. Burgess. *Chem. Soc. Rev.* **2013**, *42*, 77–88.
- [3] G. Baryshnikov, B. Minaev, H. Ågren. *Chem. Rev.* **2017**, *117*, 6500–6537.
- [4] C. K. Prier, D. A. Rankic, D. W. C. MacMillan. *Chem. Rev.* **2013**, *113*, 5322–5363.
- [5] D. P. Hari, B. König. *Angew. Chem. Int. Ed.* **2013**, *52*, 4734–4743.
- [6] D. Ravelli, M. Fagnoni, A. Albini. *Chem. Soc. Rev.* **2013**, *42*, 97–113.
- [7] L. Shi, W. Xia. *Chem. Soc. Rev.* **2012**, *41*, 7687–7697.
- [8] K. Aryanpour, J. A. Muñoz, S. Mazumdar. *J. Phys. Chem. C* **2013**, *117*, 4971–4979.
- [9] T. N. Singh-Rachford, F. N. Castellano. *Coord. Chem. Rev.* **2010**, *254*, 2560–2573.
- [10] C. Ye, L. Zhou, X. Wang, Z. Liang. *Phys. Chem. Chem. Phys.* **2016**, *18*, 10818–10835.
- [11] A. Monguzzi, R. Tubino, S. Hoseinkhani, M. Campione, F. Meinardi. *Phys. Chem. Chem. Phys.* **2012**, *14*, 4322–4332.
- [12] J. Zhao, W. Wu, J. Sun, S. Guo. *Chem. Soc. Rev.* **2013**, *42*, 5323–5351.
- [13] N. J. Turro, V. Ramamurthy, J. C. Scaiano, *Principles of Molecular Photochemistry: An Introduction*, University Science Books: Sausalito, California, **2009**.
- [14] M. Bröring, R. Krüger, S. Link, C. Kleeberg, S. Köhler, X. Xie, B. Ventura, L. Flamigni. *Chem.–Eur. J.* **2008**, *14*, 2976–2983.
- [15] A. Harriman, L. J. Mallon, G. Ulrich, R. Ziessel. *ChemPhysChem* **2007**, *8*, 1207–1214.
- [16] G. P. Wiederrecht, W. A. Svec, M. R. Wasielewski, T. Galili, H. Levanon. *J. Am. Chem. Soc.* **2000**, *122*, 9715–9722.
- [17] L. Huang, X. Cui, B. Therrien, J. Zhao. *Chem.–Eur. J.* **2013**, *19*, 17472–17482.
- [18] L. Huang, X. Yu, W. Wu, J. Zhao. *Org. Lett.* **2012**, *14*, 2594–2597.
- [19] S. M. Dyar, E. A. Margulies, N. E. Horwitz, K. E. Brown, M. D. Krzyaniak, M. R. Wasielewski. *J. Phys. Chem. A* **2015**, *119*, 13560–13569.
- [20] Y. Teki, S. Miyamoto, M. Nakatsuji, Y. Miura. *J. Am. Chem. Soc.* **2001**, *123*, 294–305.
- [21] Z. E. X. Dance, S. M. Mickley, T. M. Wilson, A. B. Ricks, A. M. Scott, M. A. Ratner, M. R. Wasielewski. *J. Phys. Chem. A* **2008**, *112*, 4194–4201.
- [22] M. A. Filatov, S. Karuthedath, P. M. Polestshuk, H. Savoie, K. J. Flanagan, C. Sy, E. Sitte, M. Telitchko, F. Laquai, R. W. Boyle, M. O. Senge. *J. Am. Chem. Soc.* **2017**, *139*, 6282–6285.
- [23] X. Zhang, N. Feng. *Chem.–Asian J.* **2017**, *12*, 2447–2456.
- [24] K. Chen, W. Yang, Z. Wang, A. Iagatti, L. Bussotti, P. Foggi, W. Ji, J. Zhao, M. Di Donato. *J. Phys. Chem. A* **2017**, *121*, 7550–7564.
- [25] Z. Wang, J. Zhao. *Org. Lett.* **2017**, *19*, 4492–4495.

RESEARCH ARTICLE

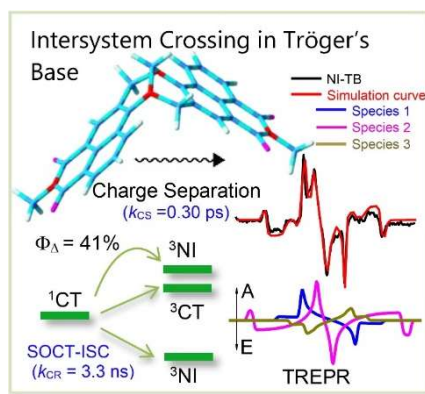
- [26] M. A. Filatov, S. Karuthedath, P. M. Polestshuk, S. Callaghan, K. J. Flanagan, M. Telitchko, T. Wiesner, F. Laquai, M. O. Senge. *Phys. Chem. Chem. Phys.* **2018**, *20*, 8016–8031.
- [27] Y. Zhao, R. Duan, J. Zhao, C. Li. *Chem. Commun.* **2018**, *54*, 12329–12332.
- [28] Y. Hou, T. Biskup, S. Rein, Z. Wang, L. Bussotti, N. Russo, P. Foggi, J. Zhao, M. Di Donato, G. Mazzone, S. Weber. *J. Phys. Chem. C* **2018**, *122*, 27850–27865.
- [29] B. Dolenský, J. Elguero, V. Král, C. Pardo, M. Valík. *Adv. Heterocycl. Chem.* **2007**, *93*, 1–56.
- [30] C. Yuan, X. Tao, L. Wang, J. Yang, M. Jiang. *J. Phys. Chem. C* **2009**, *113*, 6809–6814.
- [31] E. B. Veale, T. Gunnlaugsson. *J. Org. Chem.* **2010**, *75*, 5513–5525.
- [32] E. M. Boyle, S. Comby, J. K. Molloy, T. Gunnlaugsson. *J. Org. Chem.* **2013**, *78*, 8312–8319.
- [33] Z. Kejík, T. Bříza, M. Havlík, B. Dolenský, R. Kaplánek, J. Králová, I. Mikula, P. Martásek, V. Král. *Dyes Pigments* **2016**, *134*, 212–218.
- [34] I. Neogi, S. Jhulki, A. Ghosh, T. J. Chow, J. N. Moorthy. *ACS Appl. Mater. Inter.* **2015**, *7*, 3298–3305.
- [35] N. R. Deprez, K. A. McNitt, M. E. Petersen, R. G. Brown, D. E. Lewis. *Tetrahedron Lett.* **2005**, *46*, 2149–2153.
- [36] E. B. Veale, D. O. Frimannsson, M. Lawler, T. Gunnlaugsson. *Org. Lett.* **2009**, *11*, 4040–4043.
- [37] S. Banerjee, S. A. Bright, J. A. Smith, J. Burgeat, M. Martinez-Calvo, D. C. Williams, J. M. Kelly, T. Gunnlaugsson. *J. Org. Chem.* **2014**, *79*, 9272–9283.
- [38] S. Shanmugaraju, C. Dabadie, K. Byrne, A. J. Savyasachi, D. Umadevi, W. Schmitt, J. A. Kitchen, T. Gunnlaugsson. *Chem. Sci.* **2017**, *8*, 1535–1546.
- [39] B. Wilson, M.-J. Fernández, A. Lorente, K. B. Grant. *Tetrahedron* **2008**, *64*, 3429–3436.
- [40] S. Murphy, S. A. Bright, F. E. Poynton, T. McCabe, J. A. Kitchen, E. B. Veale, D. C. Williams, T. Gunnlaugsson. *Org. Biomol. Chem.* **2014**, *12*, 6610–6623.
- [41] S. Shanmugaraju, B. la Cour Poulsen, T. Arisa, D. Umadevi, H. L. Dalton, C. S. Hawes, S. Estalayo-Adrián, A. J. Savyasachi, G. W. Watson, D. C. Williams, T. Gunnlaugsson. *Chem. Commun.* **2018**, *54*, 4120–4123.
- [42] E. Vauthey. *ChemPhysChem* **2012**, *13*, 2001–2011.
- [43] M. Kasha, H. R. Rawls, M. A. El-Bayoumi. *Pure Appl. Chem.* **1965**, *11*, 371–392.
- [44] D. M. P. Aroche, J. M. Toldo, R. R. Descalzo, P. F. B. Gonçalves, F. S. Rodembusch. *New J. Chem.* **2015**, *39*, 6987–6996.
- [45] X. Liu, Q. Qiao, W. Tian, W. Liu, J. Chen, M. J. Lang, Z. Xu. *J. Am. Chem. Soc.* **2016**, *138*, 6960–6963.
- [46] J. R. Lakowicz, *Principles of Fluorescence Spectroscopy*, 2nd ed., Kluwer Academic/Plenum Publishers: New York, **1999**.
- [47] C. L. Ramírez, C. Pegoraro, L. Trupp, A. Bruttomesso, V. Amorebieta, D. M. A. Vera, A. R. Parise. *Phys. Chem. Chem. Phys.* **2011**, *13*, 20076–20080.
- [48] F. Han, L. Chi, W. Wu, X. Liang, M. Fu, J. Zhao. *J. Photochem. Photobiol. A* **2008**, *196*, 10–23.
- [49] J. J. Piet, W. Schuddeboom, B. R. Wegewijs, F. C. Grozema, J. M. Warman. *J. Am. Chem. Soc.* **2001**, *123*, 5337–5347.
- [50] J. M. Giaimo, A. V. Gusev, M. R. Wasielewski. *J. Am. Chem. Soc.* **2002**, *124*, 8530–8531.
- [51] S. Weber, Transient EPR. *eMagRes.* **2017**, *6*, 255–270.
- [52] H. van Willigen, G. Jones, M. S. Farahat. *J. Phys. Chem.* **1996**, *100*, 3312–3316.
- [53] Y. Cakmak, S. Kolemen, S. Duman, Y. Dede, Y. Dolen, B. Kilic, Z. Kostereli, L. T. Yildirim, A. L. Dogan, D. Guc, E. U. Akkaya. *Angew. Chem., Int. Ed.* **2011**, *50*, 11937–11941.
- [54] S. Callaghan, M. A. Filatov, H. Savoie, R. W. Boyle, M. O. Senge. *Photochem. Photobiol. Sci.* **2019**, *18*, 495–504.
- [55] A. Samanta, B. Ramachandram, G. Saroja. *J. Photochem. Photobiol. A* **1996**, *101*, 29–32.
- [56] Z. Wang, A. A. Sukhanov, A. Toffoletti, F. Sadiq, J. Zhao, A. Barbon, V. K. Voronkova, B. Dick. *J. Phys. Chem. C* **2018**, *123*, 265–274.
- [57] S. Richert, G. Bullard, J. Rawson, P. J. Angiolillo, M. J. Therien, C. R. Timmel. *J. Am. Chem. Soc.* **2017**, *139*, 5301–5304.
- [58] A. Kawai, K. Shibuya. *J. Photochem. Photobiol. C* **2006**, *7*, 89–103.
- [59] K. Möbius, W. Lubitz, A. Savitsky. *Appl. Magn. Reson.* **2011**, *41*, 113–143.
- [60] Z. E. X. Dance, Q. Mi, D. W. McCamant, M. J. Ahrens, M. A. Ratner, M. R. Wasielewski. *J. Phys. Chem. B* **2006**, *110*, 25163–25173.
- [61] Z. Wang, Y. Gao, M. Hussain, S. Kundu, V. Rane, M. Hayvali, E. A. Yildiz, J. Zhao, H. G. Yaglioglu, R. Das, L. Luo, J. Li. *Chem.–Eur. J.* **2018**, *24*, 18663–18675.
- [62] J. Atchison, S. Kamila, H. Nesbitt, K. A. Logan, D. M. Nicholas, C. Fowley, J. Davis, B. Callan, A. P. McHale, J. F. Callan. *Chem. Commun.* **2017**, *53*, 2009–2012.
- [63] I. S. Turan, F. P. Cakmak, D. C. Yildirim, R. Cetin-Atalay, E. U. Akkaya. *Chem.–Eur. J.* **2014**, *20*, 16088–16092.
- [64] A. Barbon, M. Bellinazzi, M. Casagrande, L. Storaro, M. Lenarda, M. Brustolon. *Phys. Chem. Chem. Phys.* **2006**, *8*, 5069–5078.
- [65] A. Barbon, M. Bortolus, A. Lisa Maniero, M. Brustolon. *Phys. Chem. Chem. Phys.* **2005**, *7*, 2894–2899.
- [66] A. Barbon, E. D. Bott, M. Brustolon, M. Fabris, B. Kahr, W. Kaminsky, P. J. Reid, S. M. Wong, K. L. Wustholz, R. Zanré. *J. Am. Chem. Soc.* **2009**, *131*, 11548–11557.
- [67] J. J. P. Stewart. *J. Mol. Model.* **2004**, *10*, 155–164.

RESEARCH ARTICLE

Entry for the Table of Contents

RESEARCH ARTICLE

Tröger's Base as potent triplet photosensitizer! We discovered efficient intersystem crossing in Tröger's base, a novel molecular structural motif for attaining efficient spin orbital charge transfer ISC (SOCT-ISC). The fully rigid orthogonal structure is beneficial for efficient SOCT-ISC ($\Phi_{\Delta} = 41\%$). The ISC mechanism was confirmed with time-resolved electron paramagnetic resonance spectroscopy (TREPR).



Yingjie Zhao, Kepeng Chen, Elif Akhuseyin Yildiz, Shujing Li, Yuqi Hou, Xue Zhang, Zhijia Wang, Jianzhang Zhao,* Antonio Barbon,* Halime Gul Yaglioglu* and Huijian Wu*

Page No. – Page No.

Efficient Intersystem Crossing in Tröger's Base Derived From 4-Amino-1,8-Naphthalimide and Application as Potent PDT Reagent